AJBAR Vol. 3(1), February 2024: 42-64, ISSN: 2811-2881

Arid Zone Journal of Basic and Applied Research

Faculty of Science, Borno State University Maiduguri, Nigeria

Journal homepage: https://www.azjournalbar.com

Research Article

Transient Stability Improvement on Power Network using Static Synchronous Compensator: A Case of The Nigerian 330 KV Electricity Grid

Olaogun P. O.[1], Adebisi O. I.[1], Adejumobi I. A.[1] and Adams D. O.[2]

[1]Department of Electrical and Electronics Engineering, Federal University of Agriculture, Abeokuta, Ogun State, Nigeria

[2]Department of Mathematics, Federal University of Agriculture, Abeokuta, Ogun State, Nigeria

*Corresponding author's Email: olayemiolaogunpeter@gmail.com, doi.org/10.55639/607.464544

ARTICLE INFO:

Keywords:
Modified Euler,
Newton- Rapson,
Power flow,
STATCOM,
Transient stability

ABSTRACT

This study deals with power system transient stability, enhanced via a static synchronous compensator (STATCOM). The system's steady state and transient responses were modelled with Newton-Raphson-based power flow and modified Euler-based swing equation, respectively. Simulations were performed with and without STATCOM, considering the Nigerian 34-bus power grid. A balanced three-phase fault was used for the transient stability analysis. The voltage magnitudes of Katampe (0.9373), Kaduna (0.9209), Kano (0.9381), Jos (0.8295), and Gombe (0.7795) in the grid violated the statutory voltage limit of 0.95 to 1.05 p.u. before compensation and were improved to 0.9650, 0.9550, 0.9789, 0.9630, and 0.9550 p.u., respectively after STATCOM was applied. The system's total real line losses before and after compensation were 57.887 and 55.623 MW, respectively. Fault application on bus 20 (Akangba T.S) caused loss of synchronism on generator 14 when the critical fault clearing time (CFCT) exceeded 0.019 s while generators 2 to 13 experienced marginal stability. The STATCOM application restored stability beyond the CFCT of 0.019 s due to compensation provided by the device. Fault introduction on bus 22 drove Egbin, the largest system's generator corresponding to generator 7 on the swing curve into marginal stability along with generators 3 to 6 and 8 to 14 while generator 2 lost synchronism beyond a fault CFCT of 0.0130 s. However, the STATCOM application restored the system's stability. STATCOM aided the transient stability improvement of the Nigerian 34-bus power network for effective operation.

Corresponding author: Olaogun P. O, **Email:** olayemiolaogunpeter@gmail.com
Department of Electrical and Electronics Engineering, Federal University of Agriculture, Abeokuta, Ogun State, Nigeria

INTRODUCTION

In this modern era of technological innovations, the complexity of power system networks has tremendously increased with many diverse components interconnected to provide electricity to service the customer's needs (Azeez & Abdelfattah, 2020; Garg et al., 2017; Hadi, 2008; Murali et al., 2010). The existing transmission system is being overburdened than the initially designed capacity due to the ever-growing demand for electrical energy (Kumar & Nagaraju, 2007; Shrivastava et al., 2021). The persistent long transmission line loading increase to match the energy needs of the customers has made transient instability an important consideration in the transfer of electrical energy after a major disturbance such as sudden load addition, faults, loss of generation, loss of large loads, and sudden disconnection of lines occurs (Braide & Diema, 2018; Eidiani *et al.,* 2011). This has resulted in multiple outages, downtimes, and economic and technical losses experienced in electric power transmission grids.

Transient stability, simply put, is the power system's ability to maintain synchronism or stable operation after experiencing severe or large disturbance (Kothari & Nagrath, 2008; Okakwu & Ogujor, 2017). The control of transient instability is extremely important for the effective operation of power system networks (Garg *et al.*, 2017; K. Gupta & Pahariya, 2017; Murali et al., 2010). Initially, the effect of transient disturbances was managed by the conventional method involving the use of mechanical switches. However, the effectiveness of this control technique is hindered by its possible mechanical components' wear and tear, huge maintenance cost, and time delay (Garg *et al.*, 2017; Padiyar & Rao, 1999). An alternative solution to overcome the challenges of mechanical switches involves the creation of more generation plants and transmission networks; nevertheless, this exercise also comes with its demerits. It is time-consuming and capital-intensive, and there may arise possible environmental challenges (Jokojeje et al., 2015a; Qader, 2015). These shortcomings of the conventional techniques led to the control of transient instability in electricity grids via flexible alternating current transmission systems (FACTS) application.

FACTS, as described by the Institute of Electrical and Electronics Engineers, are solid state and other static controllers with the capacity to control and increase power transfer of the alternating current transmission systems (Singh et al., 2012; Udo & Aminu, 2019). FACTS technology has widespread acceptance because of its quick action, cost-effectiveness, and ability to improve system reliability, security, and efficiency (Adebisi *et al.*, 2018; Jokojeje et al., 2015b, Asare *et al.,* 1994). FACTS family comprises many members with popular ones being unified Power flow controller (UPFC), static synchronous series capacitor (SSSC), thyristor controlled series capacitor (TCSC), static var compensator (SVC), static synchronous compensator (STATCOM), among others (Anichebe & Ekwue, 2020; Eladany *et al.*, 2018; Khan et al., 2017; Murali *et al.*, 2010; Ramana & Ram, 2011; Singh *et al.*, 2012). Each of these controllers has their uniqueness which makes them fit suitably into the specific applications where they are deployed.

Therefore, the goal of this study was to employ STATCOM for power system transient stability improvement considering the Nigerian 330 kV electricity grid. The Nigerian electricity grid which comprises complex interconnections of varieties of essential equipment is currently overstressed due to excessive electrical energy demand warranted by the persistently increasing population and industrialization (Adebisi et al., 2018; Akpojedje & Ogujor, 2021; Igwilo *et al.*, 2021). Occurrence of transient disturbances such as faults, rapid load changes, switching operations and loss of components on the system already operating near its stability limit is inevitable and this usually lead to severe loss of

synchronism on the generators with the end result being voltage collapse in the entire network. This event poses major threat to the socio-economic and technological development of the end-users and can affect the progress of Nigeria as a nation. Hence, the need to enhance transient stability on the Nigerian electricity grid using appropriate compensating devices such as STATCOM which offers fast-response and economic advantages over the conventional transient control schemes such as generator excitation regulation, synchronous generator, and series compensation capacitor among others becomes highly imperative. STATCOM is a versatile member of the FACTS family with the potentials for voltage regulation and transient stability improvement as a result of its small size requirement, lower generation of harmonics and effective control action (Gupta & Tripathi, 2015; Mumtahina et al., 2023).

METHODOLOGY

Power Flow Formulation

Power flow is a key tool in the design and analysis of power systems. It is very crucial for power system planning and operation, power transfer between utilities, economic scheduling, contingency, and transient stability studies (Gupta, 2011; Hadi, 2008; Kothari & Nagrath, 2008). Power flow in this study was formulated with the consideration of a typical power system bus arrangement shown in Figure 1.

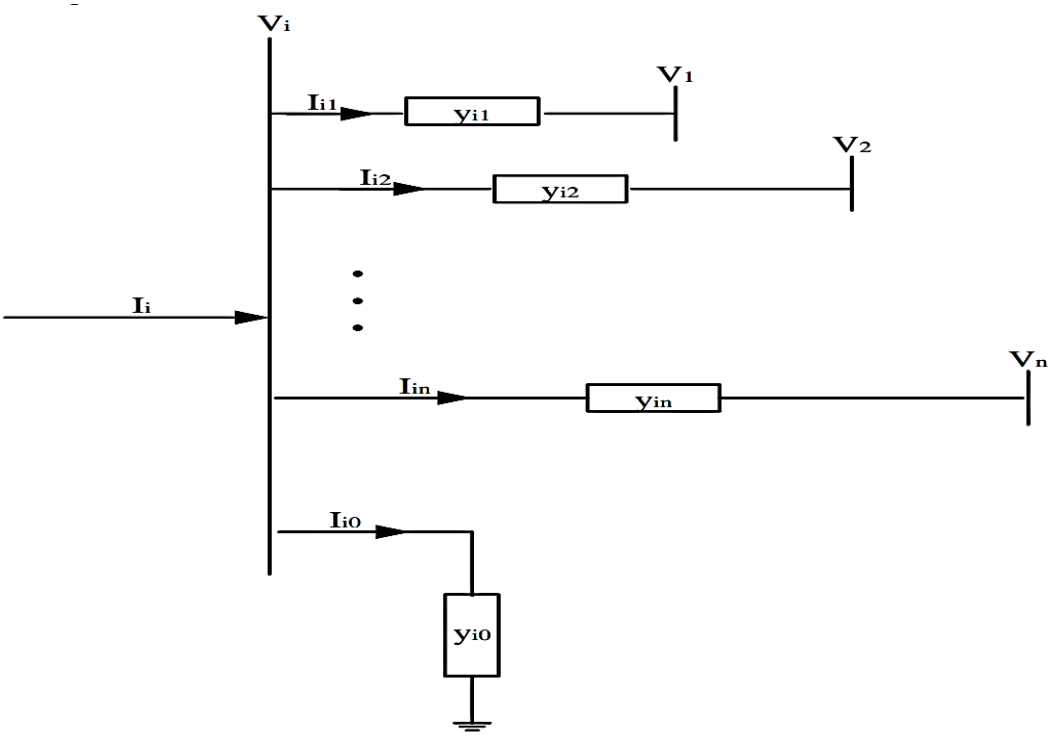

Figure 1: An n-bus structure of power system (Gupta, 2011; Hadi, 2008; Kothari and Nagrath, 2008)

Application of KCL to the bus system in Figure 1 yields equation (1) which modifies into equations (2) and (3) with further application of KVL and algebraic manipulation respectively:

$$I_i = I_{i0} + I_{i1} + I_{i2} + \cdots + I_{in} \quad (1)$$

$$I_i = y_{i0}V_i + y_{i1}(V_i - V_1) + y_{i2}(V_i - V_2) + \cdots + y_{in}(V_i - V_n) \quad (2)$$

$$I_i = (y_{i0} + y_{i1} + y_{i2} + \cdots + y_{in})V_i - y_{i1}V_1 - y_{i2}V_2 - \cdots - y_{in}V_n \quad (3)$$

Where I_i is the current injected into bus *i*
I_{i0} is the current flowing from bus *i* to ground
I_{i1} is the current flowing from bus *i* to bus 1
I_{i2} is the current flowing from bus *i* to bus 2
I_{in} is the current flowing from bus *i* to bus n
V_i is voltage at bus *i*
V_1 is the voltage at bus 1
V_2 is the voltage at bus 2
V_n is the voltage at bus n
y_{i0} is the admittance of transmission line between bus i and ground
y_{i1} is the admittance of transmission line between bus i and bus 1
y_{i2} is admittance of transmission line between bus i and bus 2
y_{in} is admittance of transmission line between bus i and bus n

Further simplification of equation (3) with definition given by equation (4) results in equation (5) with a modification expressed by equations (6) and (7):

$$\begin{cases} Y_{ii} = y_{i0} + y_{i1} + y_{i2} + \cdots + y_{in} \\ Y_{i1} = -y_{i1} \\ Y_{i2} = -y_{i2} \\ \vdots \quad \vdots \quad \vdots \\ Y_{in} = -y_{in} \end{cases} \quad (4)$$

$$I_i = Y_{ii}V_i + Y_{i1}V_1 + Y_{i2}V_2 + \cdots + Y_{in}V_n \quad (5)$$

$$I_i = \sum_{j=1}^{n} Y_{ij}V_j \quad (6)$$

$$I_i = \sum_{j=1}^{n} |Y_{ij}||V_j| \angle \theta_{ij} + \delta_j \quad (7)$$

Where I_i, V_i, y_{ij}, Y_{ij}, V_j, $|Y_{ij}|$, $|V_j|$, θ_{ij} and δ_j respectively denote the supplied current at bus *i*, the voltage at bus *i*, the admittance of line *i-j*, the element of bus admittance derived from admittance of line *i-j*, the voltage of bus *j*, the magnitude of admittance of line *i-j*, the magnitude of voltage at bus *j*, the angle of admittance of line *i-j*, and the angle of voltage at bus *j*.

Expansion of equation (6) for *i* equals to 1 to n produces equation (8) with Y_{bus} given by the matrix of equation (9):

$$\begin{bmatrix} I_1 \\ I_2 \\ \vdots \\ I_n \end{bmatrix} = \begin{bmatrix} Y_{11} & Y_{12} & \cdots & Y_{1n} \\ Y_{21} & Y_{22} & \cdots & Y_{2n} \\ \vdots & \vdots & \vdots & \vdots \\ Y_{n1} & Y_{2n} & \cdots & Y_{nn} \end{bmatrix} \begin{bmatrix} V_1 \\ V_2 \\ \vdots \\ V_n \end{bmatrix} \quad (8)$$

$$Y_{bus} = \begin{bmatrix} Y_{11} & Y_{12} & \cdots & Y_{1n} \\ Y_{21} & Y_{22} & \cdots & Y_{2n} \\ \vdots & \vdots & \vdots & \vdots \\ Y_{n1} & Y_{2n} & \cdots & Y_{nn} \end{bmatrix} \quad (9)$$

The power supplied at bus *i* takes an expression of equation (10) which produces equations (11) and (12) after substitution of equation (7) and decomposition into real and imaginary components:

$$P_i - jQ_i = V_i^* I_i \quad (10)$$

$$P_i = \sum_{j=1}^{n} |V_i||V_j||Y_{ij}| cos(\theta_{ij} + \delta_{ij}) \quad (11)$$

$$Q_i = -\sum_{j=1}^{n} |V_i||V_j||Y_{ij}| sin(\theta_{ij} + \delta_{ij}) \quad (12)$$

With $\delta_{ij} = \delta_j - \delta_i$ (13)

Where P_i and Q_i respectively represent bus *i* active and reactive powers.

Equations (11) and (12) are the static power flow expressions that govern the steady state response of a power system. They are non-linear equations solved via numerical iterative method. These equations were implemented in this study using the Newton-Raphson method because of its faster convergence rate, accuracy, and reliability in comparison to other iterative methods (Gupta, 2011; Hadi, 2008; Kothari and Nagrath, 2008). The Newton- Raphson-based power flow equations arising from the linearization of equations (11) and (12) are expressed by equation (14):

$$\begin{bmatrix} \Delta P \\ \Delta Q \end{bmatrix} = \begin{bmatrix} J_1 & J_2 \\ J_3 & J_4 \end{bmatrix} \begin{bmatrix} \Delta\delta \\ \Delta|V| \end{bmatrix} \quad (14)$$

Where J_1, J_2, J_3, and J_4 are the elements of the Jacobin matrix, ΔP, ΔQ, $\Delta\delta$ and $\Delta|V|$ are respectively active power, reactive power, bus voltage angle, and bus voltage magnitude mismatches.

ΔP, ΔQ, $\Delta\delta$, $\Delta|V|$, J_1, J_2, J_3, and J_4 are expressed by equations (15) to (22):

$$\Delta P = \begin{bmatrix} \Delta P_2^{(k)} \\ \vdots \\ \Delta P_n^{(k)} \end{bmatrix} \quad (15)$$

$$\Delta Q = \begin{bmatrix} \Delta Q_2^{(k)} \\ \vdots \\ \Delta Q_n^{(k)} \end{bmatrix} \quad (16)$$

$$\Delta\delta = \begin{bmatrix} \Delta\delta_2^{(k)} \\ \vdots \\ \Delta\delta_n^{(k)} \end{bmatrix} \quad (17)$$

$$\Delta|V| = \begin{bmatrix} \Delta\left|V_2^{(k)}\right| \\ \vdots \\ \Delta\left|V_n^{(k)}\right| \end{bmatrix} \quad (18)$$

$$J_1 = \begin{bmatrix} \frac{\partial P_2^{(k)}}{\partial \delta_2} & \cdots & \frac{\partial P_2^{(k)}}{\partial \delta_n} \\ \vdots & \ddots & \vdots \\ \frac{\partial P_n^{(k)}}{\partial \delta_2} & \cdots & \frac{\partial P_n^{(k)}}{\partial \delta_n} \end{bmatrix} \quad (19)$$

$$J_2 = \begin{bmatrix} \frac{\partial P_2^{(k)}}{\partial |V_2|} & \cdots & \frac{\partial P_2^{(k)}}{\partial |V_n|} \\ \vdots & \ddots & \vdots \\ \frac{\partial P_n^{(k)}}{\partial |V_2|} & \cdots & \frac{\partial P_n^{(k)}}{\partial |V_n|} \end{bmatrix} \quad (20)$$

$$J_3 = \begin{bmatrix} \frac{\partial Q_2^{(k)}}{\partial \delta_2} & \cdots & \frac{\partial Q_2^{(k)}}{\partial \delta_n} \\ \vdots & \ddots & \vdots \\ \frac{\partial Q_n^{(k)}}{\partial \delta_2} & \cdots & \frac{\partial Q_n^{(k)}}{\partial \delta_n} \end{bmatrix} \quad (21)$$

$$J_4 = \begin{bmatrix} \frac{\partial Q_2^{(k)}}{\partial |V_2|} & \cdots & \frac{\partial Q_2^{(k)}}{\partial |V_n|} \\ \vdots & \ddots & \vdots \\ \frac{\partial Q_n^{(k)}}{\partial |V_2|} & \cdots & \frac{\partial Q_n^{(k)}}{\partial |V_n|} \end{bmatrix} \quad (22)$$

The active and reactive powers mismatch at the k[th] iteration and new estimates of the bus voltage angle and magnitude are expressed respectively by equations (23) and (26):

$$\Delta P_i^{(k)} = P_i^{sch} - P_i^{(k)} \quad (23)$$

$$\Delta Q_i^{(k)} = Q_i^{sch} - Q_i^{(k)} \quad (24)$$

$$\delta_i^{(k+1)} = \delta_i^{(k)} + \Delta \delta_i^{(k)} \quad (25)$$

$$V_i^{(k+1)} = \left|V_i^{(k)}\right| + \Delta \left|V_i^{(k)}\right| \quad (26)$$

The voltage and reactive power constraints imposed at bus *i* are expressed by equations (27) and (28) respectively:

$$V_{imin} \leq V_i \leq V_{imax} \quad (27)$$

$$Q_{imin} \leq Q_i \leq Q_{imax} \quad (28)$$

Where V_{imin}, V_{imax}, Q_{imin}, and Q_{imax} respectively denote minimum voltage magnitude, maximum voltage magnitude, minimum reactive power supply, and maximum reactive power supply at bus *i*.

Swing Equation Formulation

According to Newton's second law, the motion of the rotor of a generating unit comprising a three-phase synchronous generator and its prime mover is described by equation (23) (Glover and Sarma, 2002; Kothari & Nagrath, 2008):

$$J \propto_m (t) = T_m(t) - T_e(t) = T_a(t) \quad (23)$$

Where $\propto_m$, T_m, T_e, and T_n denote rotor angular acceleration in $rad/_{S^2}$, mechanical torque of the prime mover minus retarding torque resulting from mechanical losses in Nm, electrical torque responsible for the generator's total three-phase electrical power output plus electrical losses in Nm and net accelerating torque in Nm respectively.

The angular acceleration of the rotor is expressed by equation (24) (Glover & Sarma, 2002; Kothari & Nagrath, 2008)

$$\propto_m (t) = \frac{d\omega_m}{dt} = \frac{d^2\theta_m(t)}{dt^2} \quad (24)$$

With $\omega_m(t) = \frac{d\theta_m(t)}{dt}$ (25)

Where ω_m and θ_m respectively denote the angular velocity of the rotor in $rad/_S$ and the angular position of the rotor about a stationary axis.

The operation of the generator requires that both T_m and T_e are positive while at steady-state, T_m is the same as T_e, leading to T_a and $\propto_m$ being zero and consequently resulting in a constant velocity of the rotor termed synchronous speed. T_a is positive when T_m exceeds T_e, making $\propto_m$ to be positive and therefore, leads to an increased speed of the rotor. Equally, the speed of the rotor decreases when T_m is lower than T_e. Since the angular position of the rotor is conveniently measured about a synchronously rotating reference axis unlike a stationary axis, $\theta_m(t)$ is, hence, expressed as equation (26) (Glover & Sarma, 2002; Kothari & Nagrath, 2008):

$$\theta_m(t) = \omega_{msyn}t + \delta_m(t) \quad (26)$$

Where ω_{msyn} and δ_m are respectively defined as the rotor's synchronous angular velocity in $rad/_S$ and the angular position of the rotor about a synchronously rotating reference.

The use of equations (24) and (26) in (23), produces equation (27):

$$J\frac{d^2\theta_m(t)}{dt^2} = J\frac{d^2\delta_m(t)}{dt^2} = T_m(t) - T_e(t) = T_a(t) \quad (27)$$

Multiplication of equation (27) by $\omega_m(t)$ and dividing by S_{rated} yields the generator's three-phase volt-ampere rating expressed by equation (28) which is a per-unit power quantity (Glover & Sarma, 2002; Kothari & Nagrath, 2008):

$$\frac{J}{S_{rated}}\frac{d^2\delta_m(t)}{dt^2}\omega_m(t) = \frac{(T_m(t)-T_e(t))}{S_{rated}}\omega_m(t) = \frac{P_m(t)-P_e(t)}{S_{rated}} = P_{mp.u.}(t) - P_{ep.u.}(t) = P_{ap.u.}(t) \quad (28)$$

Where $P_{mp.u.}$ and $P_{ep.u.}$ denote the prime mover's mechanical power mover minus the per unit mechanical losses and the generator's electrical power output plus the per unit electrical losses.

Combining equation (28) with a normalized inertia constant, H defined as equation (29) results in equation (30) (Glover & Sarma, 2002; Kothari & Nagrath, 2008):

$$H = \frac{J\omega_{msyn}^2}{S_{rated}} joules/_{VA} \; or \; per \; unit - seconds \quad (29)$$

$$2H\frac{\omega_m(t)}{\omega_{msyn}^2}\frac{d^2\delta_m(t)}{dt^2} = P_{mp.u.}(t) - P_{ep.u.}(t) = P_{ap.u.}(t) \quad (30)$$

Considering that the per-unit angular velocity of the rotor is defined as equation (31) and substituted into equation (30), equation (32) is obtained (Glover & Sarma, 2002; Kothari & Nagrath, 2008):

$$\omega_{p.u}(t) = \frac{\omega_m(t)}{\omega_{msyn}} \tag{31}$$

$$\frac{2H\omega_{p.u.}(t)}{\omega_{msyn}}\frac{d^2\delta_m(t)}{dt^2} = P_{mp.u.}(t) - P_{ep.u.}(t) = P_{ap.u.}(t) \tag{32}$$

Electrical angular acceleration α, electrical radian frequency ω, power angle δ of a synchronous generator with P number of poles, synchronous electrical radian frequency ω_{syn}, and per-unit electrical frequency $\omega_{p.u}(t)$ are respectively expressed as equation (33) to (37) (Glover & Sarma, 2002; Kothari & Nagrath, 2008):

$$\alpha(t) = \frac{P}{2}\alpha_m(t) \tag{33}$$

$$\omega(t) = \frac{P}{2}\omega_m(t) \tag{34}$$

$$\delta(t) = \frac{P}{2}\delta_m(t) \tag{35}$$

$$\omega_{syn} = \frac{P}{2}\omega_{msyn} \tag{36}$$

$$\omega_{p.u}(t) = \frac{\omega(t)}{\omega_{syn}} = \frac{\frac{2}{P}\omega(t)}{\frac{2}{P}\omega_{syn}} = \frac{\omega_m(t)}{\omega_{myn}} \tag{37}$$

The use of equations (35) and (36) in equation (32) results in equation (38) referred to as the per-unit swing equation.

$$\frac{2H}{\omega_{syn}}\omega_{p.u.}(t)\frac{d^2\delta(t)}{dt^2} = P_{mp.u.}(t) - P_{ep.u.}(t) = P_{ap.u.}(t) \tag{38}$$

Equation (38) is very crucial in the analysis of rotor dynamics for transient stability studies. It is a second-order ordinary differential equation in which an assumption of lossless machine and negligible damper winding torque have eliminated the damping term (proportional to $\frac{d\delta}{dt}$) (Kothari and Nagrath, 2009). The electrical power P_e in equation (38) depends on the sine of the angle δ and it is mathematically expressed as equations (39) and (40) (Kothari & Nagrath, 2008):

$$P_e = P_{max}sin\delta \tag{39}$$

$$P_e = \frac{|E||V|}{X_d}sin\delta \tag{40}$$

With $P_{max} = \frac{|E||V|}{X_d}$ (41)

Where P_{max} is the maximum electrical power
$|E|$ is the electromotive force of the generator
$|V|$ is the terminal voltage of the generator
X_d is the direct axis reactance

Using equations (39) and (40) in equation (38), equations (42) and (43) are obtained respectively:

$$\frac{2H\omega_{p.u.}(t)}{\omega_{syn}}\frac{d^2\delta(t)}{dt^2} = P_{mp.u.}(t) - P_{maxp.u.}sin\delta(t) \quad (42)$$

$$\frac{2H\omega_{p.u.}(t)}{\omega_{syn}}\frac{d^2\delta(t)}{dt^2} = P_{mp.u.}(t) - \frac{|E||V|}{X_d}sin\delta(t) \quad (43)$$

Assumption of ω_{syn} as $2\pi f$ and $\omega_{p.u.}(t)$ as unity for ease of analysis results in the swing equation expressed by equations (42) and (43) to be respectively modified as equations (44) and (45) respectively:

$$\frac{H}{\pi f}\frac{d^2\delta(t)}{dt^2} = P_{mp.u.}(t) - P_{maxp.u.}sin\delta(t) \quad (44)$$

$$\frac{H}{\pi f}\frac{d^2\delta(t)}{dt^2} = P_{mp.u.}(t) - \frac{|E||V|}{X_d}sin\delta(t) \quad (45)$$

Swing Equation Linearization

Transient stability analysis requires that the swing equation be linearized via a numerical iterative procedure since the exact solution is unavailable in practice. Euler, modified Euler, classical Runge-Kutta, and point-to-point methods are the common numerical techniques available for swing equation linearization (Kothari & Nagrath, 2008; Ogboh et al., 2019) However, for this study, the modified Euler method (MEM) was adopted because of its simplicity and directness. MEM provides more accurate approximations of non-linear systems or functions through re-evaluation of the gradient of the line segment (Dobrushkin, 2024; Samsudin et al., 2021). MEM application for linearization of swing equation requires the transformation of equation (38) modified as equations (44) and (45) which are all second-order non-linear differential equations into two first-order linear differential equations expressed by the state variable forms given by equations (46) and (47) for ease of analysis.

$$\frac{d\delta}{dt} = \Delta\omega \quad (46)$$

$$\frac{d\Delta\omega}{dt} = \frac{\pi f}{H}P_a \quad (47)$$

Application of MEM to equations (46) and (47) produces equations (48) to (53):

$$\delta_{i+1}^{p} = \delta_i + \frac{d\delta}{dt}\Big|_{\Delta\omega_i}\Delta t \quad (48)$$

$$\Delta\omega_{i+1}^{p} = \Delta\omega_i + \frac{d\Delta\omega}{dt}\Big|_{\delta_i}\Delta t \quad (49)$$

$$\frac{d\delta}{dt}\Big|_{\Delta\omega_{i+1}^{p}} = \Delta\omega_{i+1}^{p} \quad (50)$$

$$\left.\frac{d\Delta\omega}{dt}\right|_{\delta_{i+1}^{p}} = \frac{\pi f}{H} P_a \Big|_{\delta_{i+1}^{p}} \quad (51)$$

$$\delta_{i+1}^{c} = \delta_i + \left(\frac{\left.\frac{d\delta}{dt}\right|_{\Delta\omega_i} + \left.\frac{d\delta}{dt}\right|_{\Delta\omega_{i+1}^{p}}}{2} \right) \Delta t \quad (52)$$

$$\Delta\omega_{i+1}^{c} = \Delta\omega_i + \left(\frac{\left.\frac{d\Delta\omega}{dt}\right|_{\delta_i} + \left.\frac{d\Delta\omega}{dt}\right|_{\delta_{i+1}^{p}}}{2} \right) \Delta t \quad (53)$$

Where p is the predicted value of the involved parameters at the specified iteration and c is the corrected value of the involved parameters at the specified iteration which is obtained from the average of the two derivatives as indicated in equations (52) and (53) respectively.

Power Flow Model of STATCOM for Transient Stability Improvement

The power flow equations that guide the operation of STATCOM as a var source were formulated for this study by considering the Thevenin's equivalent circuit of the device when shunt-connected to the bus *i* in Figure 1.

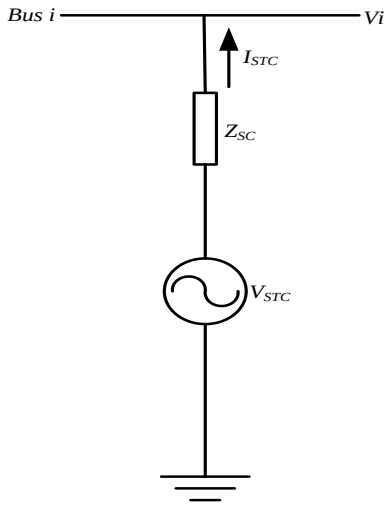

Figure 2: Thevenin's equivalent circuit of STATCOM (Jokojeje et al., 2015a; Jokojeje et al., 2015b)

The net active and reactive powers at bus *i* are given by equations (54) and (55) respectively:

$$P_i = P_{gi} + P_{STCi} - P_{li} \quad (54)$$

$$Q_i = Q_{gi} - Q_{STCi} - Q_{li} \quad (55)$$

Where P_i is the net active power at bus *i*
P_{gi} is the active power supply at bus *i*
P_{li} is the active power demand at bus *i*
P_{STCi} is the active power injected by STATCOM at bus *i*
Q_i is the net reactive power at bus *i*

Q_{gi} is the reactive power supply at bus *i*
Q_{li} is the reactive power demand at bus *i*
Q_{STCi} is the reactive power injected by STATCOM at bus *i*

The voltage and current supplied by STATCOM with the voltage constraint are given by equations (56) to (59):

$$V_{STC} = V_i + Z_{SC} I_{STC} \quad (56)$$

$$I_{STC} = I_N - Y_{SC} V_i \quad (57)$$

$$I_N = Y_{SC} V_{STC} \quad (58)$$

$$V_{STC\,min} \leq V_{STC} \leq V_{STC\,max} \quad (59)$$

Where V_{STC} is the voltage supplied by STATCOM
I_{STC} is the current supplied by STATCOM
Z_{SC} is the transformer's impedance
I_N is the Norton's current,
Y_{SC} is the short-circuit admittance
V_{STCmin} is the minimum STATCOM's voltage
V_{STCmax} is the maximum STATCOM's voltage

The power generated by STATCOM and the net power supplied into bus *i* are respectively given by equations (60) and (61):

$$S_{STC} = V_{STC} I_{STC}^* = V_{STC}^2 Y_{SC}^* - V_{STC} Y_{SC}^* V_i^* \quad (60)$$

$$S_i = V_i I_{STC}^* = V_{STC} Y_{SC}^* V_i^* - V_i^2 Y_{SC}^* \quad (61)$$

Where S_{STC} is the STATCOM's apparent power
I_{STC}^* is the complex conjugate of STATCOM's current
Y_{SC}^* is the complex conjugate of short-circuit admittance

The algebraic manipulation of equations (60) and (61) with the use of V_i and V_{STC}expressed by rectangular coordinates forms given by equations (62) and (63) results in the active and reactive power expressions represented by equations (64) to (67) for STATCOM and the system respectively.

$$V_i = e_i + jf_i \quad (62)$$

$$V_{STC} = e_{STC} + jf_{STC} \quad (63)$$

$$P_{STC} = G_{SC}\{(e_{STC}^2 + f_{STC}^2) - (e_{STC} e_i + f_{STC} f_i)\} + B_{SC}(e_{STC} f_i - f_{STC} e_i) \quad (64)$$

$$Q_{STC} = G_{SC}\{(e_{STC} e_i - f_{STC} f_i)\} + B_{SC}(-e_{STC}^2 - f_{STC}^2 + e_{STC} e_i + f_{STC} f_i) \quad (65)$$

$$P_i = G_{SC}\{e_i^2 + f_i^2 - (e_i e_{STC} + f_i f_{STC})\} + B_{SC}(e_i f_{STC} - f_i e_{STC}) \quad (66)$$

$$Q_i = G_{SC}(e_i f_{STC} - f_i e_{STC}) + B_{SC}\{(e_i f_{STC} + f_i e_{STC}) - (e_i^2 + f_i^2)\} \quad (67)$$

Where e_i is the real component of the system's voltage
f_i is the imaginary component of system's voltage
e_{STC} is the real component of the STATCOM's voltage
f_{STC} is the imaginary component of the STATCOM's voltage
P_{STC} is the STATCOM's active power
Q_{STC} is the STATCOM's reactive power
G_{SC} is the short-circuit conductance
B_{SC} is the short short-circuit susceptance

The Newton-Raphson linearized set of power flow equations based on equations (62), (64), (65) and (66) are expressed by the matrix of equation (23):

$$\begin{bmatrix} \Delta P_i \\ \Delta |V_i|^2 \\ \Delta P_{STC} \\ \Delta Q_{STC} \end{bmatrix} = \begin{bmatrix} \frac{\partial P_i}{\partial e_i} & \frac{\partial P_i}{\partial f_i} & \frac{\partial P_i}{\partial e_{STC}} & \frac{\partial P_i}{\partial f_{STC}} \\ \frac{\partial |V_i|^2}{\partial e_i} & \frac{\partial |V_i|^2}{\partial f_i} & 0 & 0 \\ \frac{\partial P_{STC}}{\partial e_i} & \frac{\partial P_{SCT}}{\partial f_i} & \frac{\partial P_{STC}}{\partial e_{STC}} & \frac{\partial P_{STC}}{\partial f_{STC}} \\ \frac{\partial Q_{STC}}{\partial e_i} & \frac{\partial Q_{SCT}}{\partial f_i} & \frac{\partial Q_{STC}}{\partial e_{STC}} & \frac{\partial Q_{STC}}{\partial f_{STC}} \end{bmatrix} \begin{bmatrix} \Delta e_i \\ \Delta f_i \\ \Delta e_{STC} \\ \Delta e_{STC} \end{bmatrix} \quad (68)$$

The STATCOM's operation for transient's stability improvement of transient stability can be described with three scenarios of the swing equation (Kakaiya & Parekh, 2019):

Scenario 1: When $P_m = P_e$, the accelerating power is zero and the system is in a steady state.

Scenario 2: When $P_m > P_e$, the rotor accelerates due to large load loss.

Scenario 3: When $P_m < P_e$, the rotor's acceleration decreases as a result of a three-phase fault occurrence.

For the control of the machine's output power, when H changes, the accelerating power is controlled with the limits. If scenario 2 occurs, the machine accelerates and the STATCOM generates a voltage and introduces a capacitive reactance in the line. However, for scenario 3, the machine experiences retardation, and STATCOM operates in such a way that it produces a voltage that causes inductive reactance to be introduced into the line for the system's balanced operation.

Test Network and Simulation

The Nigerian 330 kV, 14-machine, 34-bus power network whose one-line diagram and data were sourced from National Control Centre of the Transmission Company of Nigeria and detailed in the work of Ikeli (2019) were considered as a test case for this study. Figure 2 shows the one-line of the network while the data are provided in Appendices I-III. Direct coding via MATLAB was employed for the load flow and transient stability simulations of the network in Figure 2 due to MATLAB's robustness and capability for the manipulation of mathematical algorithms. The network's bus, branch and generator data along with STATCOM's rating were used as inputs during simulations. A balanced three-phase short-circuit was introduced on some buses and the system responses in the event of the transient disturbance with and without compensation via STATCOM were observed. The critical fault

clearing times were determined from the responses.

RESULTS AND DISCUSSION

Nigerian 34-Bus Network Load Flow Results

The results of the Nigerian 34-bus network load flow study before transient stability analysis and enhancement are delineated in Figures 3 and 4 which respectively represent the system voltage profile and total active line loss. Figure 3 revealed that five buses violated the voltage statutory limit of 0.95 to 1.05 p.u. The buses which are Katampe (6), Kaduna T.S (10), Kano T.S (13), Jos T.S (14), and Gombe T.S (17) had voltage magnitudes of 0.9373, 0.9209, 0.9381, 0.8295 and 0.7795 respectively. The STATCOM application on the system enhanced the voltage magnitudes of Katampe, Kaduna T.S, Kano T.S, Jos, and Gombe to 0.9650, 0.9550, 0.97890, 0.9630 and 0.9550 p.u. respectively. The system's total active power loss before compensation from Figure 4 was 57.887 MW and reduced to 55.623 MW after compensation.

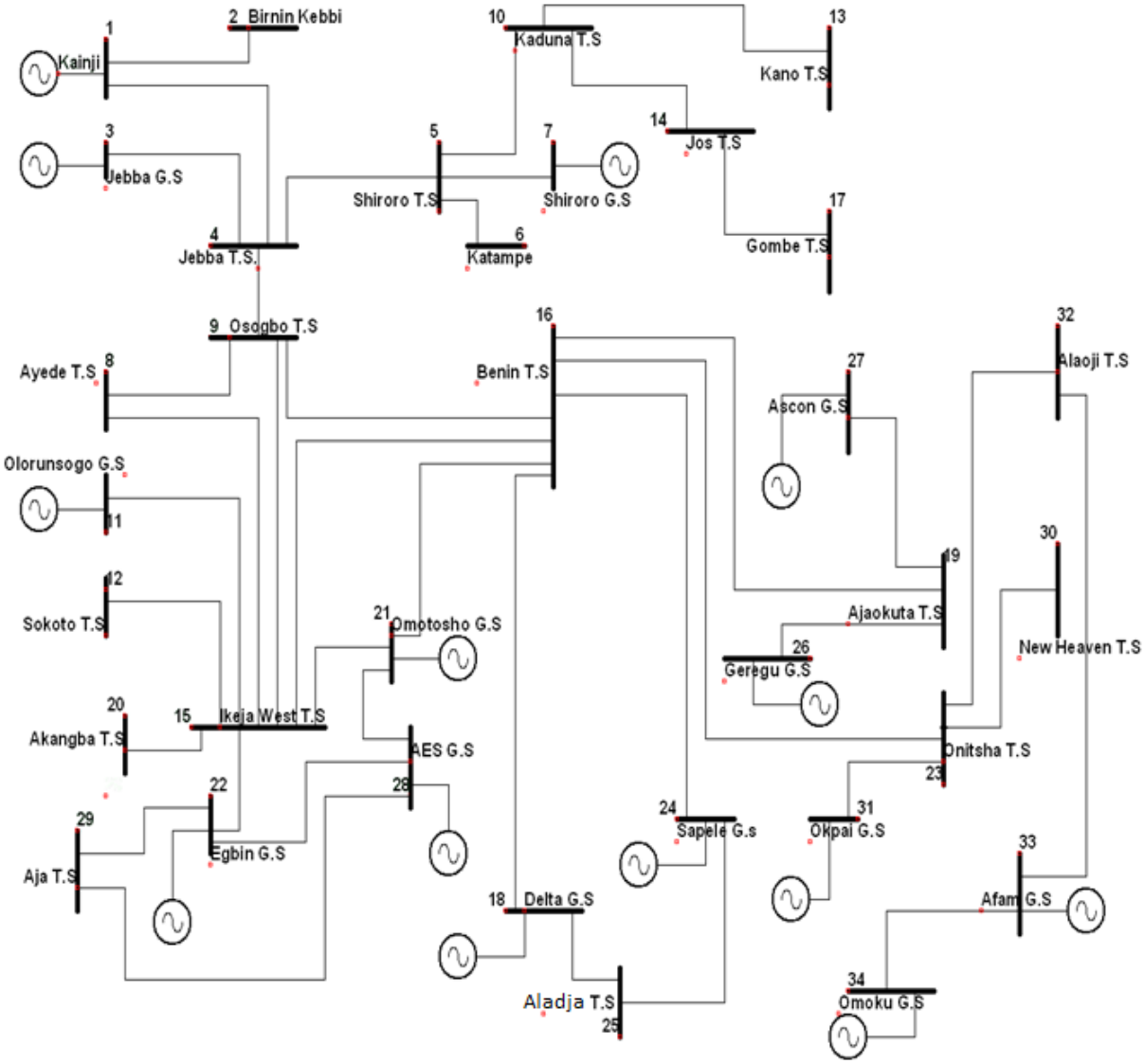

Figure 2: Nigerian 14-machine, 34-bus power network (Ikeli, 2019)

The voltage violations observed on the critical buses before the application of compensation indicated that the considered network was operating ineffectively and the instability due to the observed undervoltage conditions could negatively affect the security margin of the system, thereby, causing among others blackouts, equipment damage and high losses. The high losses potentially reduce the useful electrical energy that could have been transported on the network to address more customers' needs. The STATCOM's application, however, stabilized the system bus voltages and minimized the power losses.

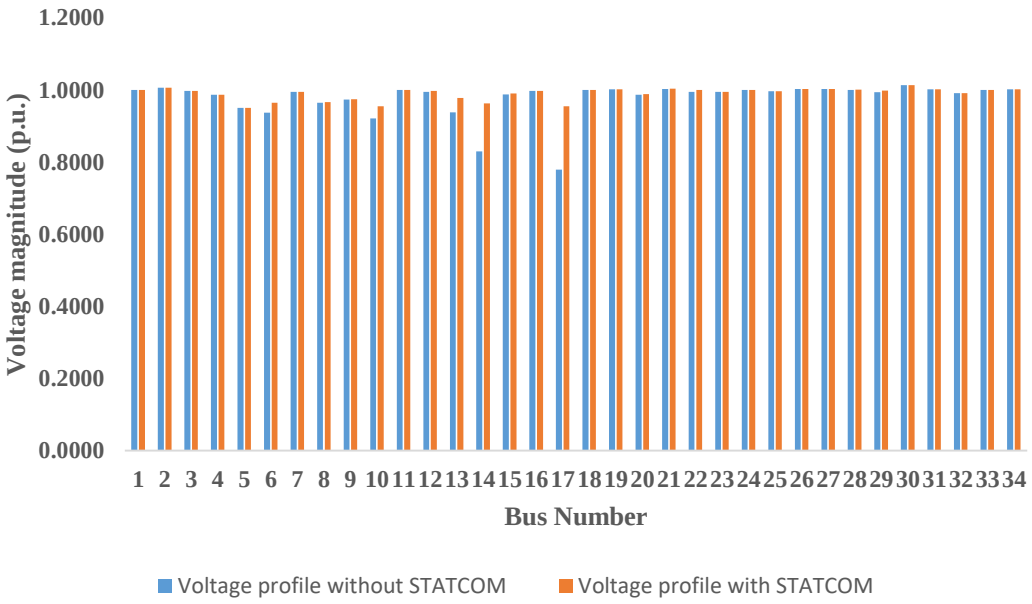

Figure 3: Voltage magnitudes of the Nigerian 34-bus power network

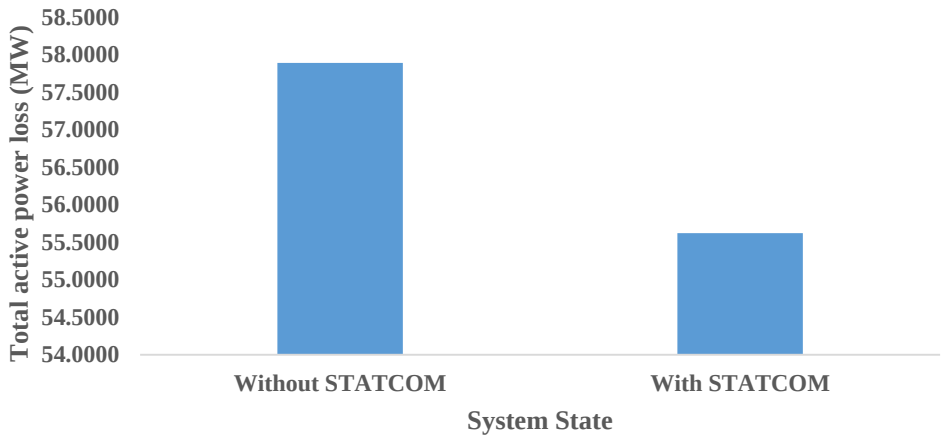

Figure 4: Total active power loss of the Nigerian 34-bus power network

Nigerian 34-Bus Network Transient Stability Analysis and Enhancement Results

Transient Stability Results for Three-Phase Fault on Bus 20, Line [15-20]

The swing curves of the generators in the Nigerian 34-bus power network for a three-phase short circuit fault introduced on bus 20, line [15-20] and cleared at different times with and without STATCOM are presented in Figures 6 to 8. Figures 6a and b showed that the system was stable at a fault clearing time (FCT) of 0.019 s with and without enhancement. However, the stability was negatively impacted as depicted in Figure 7a by increasing the FCT to 0.020 s without STATCOM where generator 14 lost synchronism while generators 2 to 13 went into marginal stability. Full stability was, however, regained when STATCOM was included on bus 20 as shown in Figure 7b. The instability of generator 14 and marginal stability of generators 2 to 13 persisted when the FCT was increased to 0.021 s as depicted in Figure 8a. The STATCOM integration into the system restored stability as presented in Figure 8b. These results implied that the inclusion of STATCOM on the considered network was able to extend the critical fault clearing time such that loss of system's stability did not ensue at the instance of fault occurrence. This action was achieved by STATCOM via injection of reactive power which compensated var deficiency around the vicinity where fault occurrence is experienced. As a result, the negative effect of the fault was minimized and the system was stabilized through sustenance of the synchronous operation.

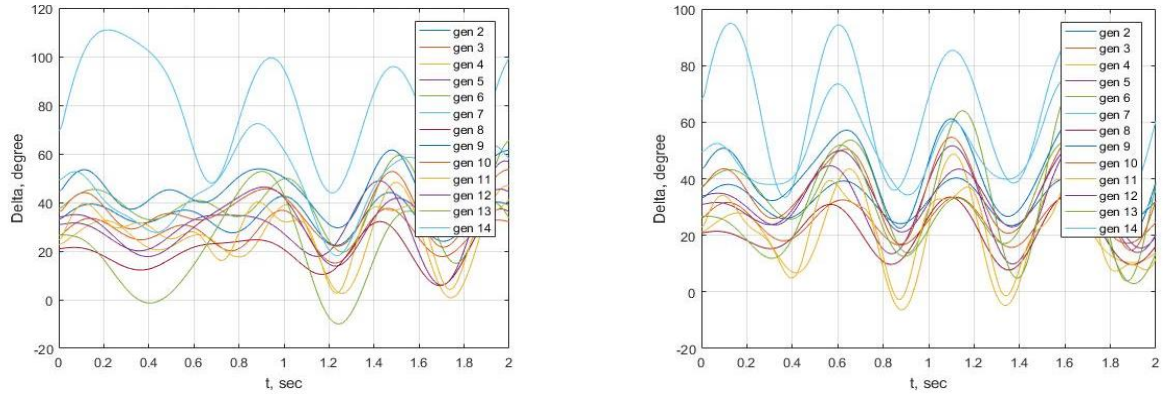

(a) (b)

Figure 6: Swing curve of three-phase fault on bus 20, line [15-20] of the Nigerian 34-bus power network and cleared at 0.019 s (a) without STATCOM (b) with STATCOM

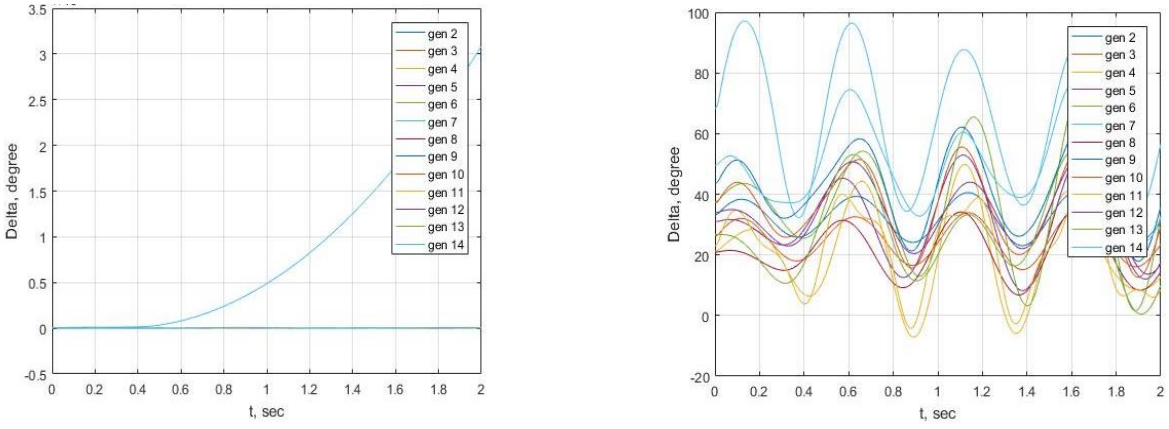

(a) (b)

Figure 7: Swing curve of three-phase fault on bus 20, line [15-20] of the Nigerian 34-power network and cleared at 0.020 s (a) without STATCOM (b) with STATCOM

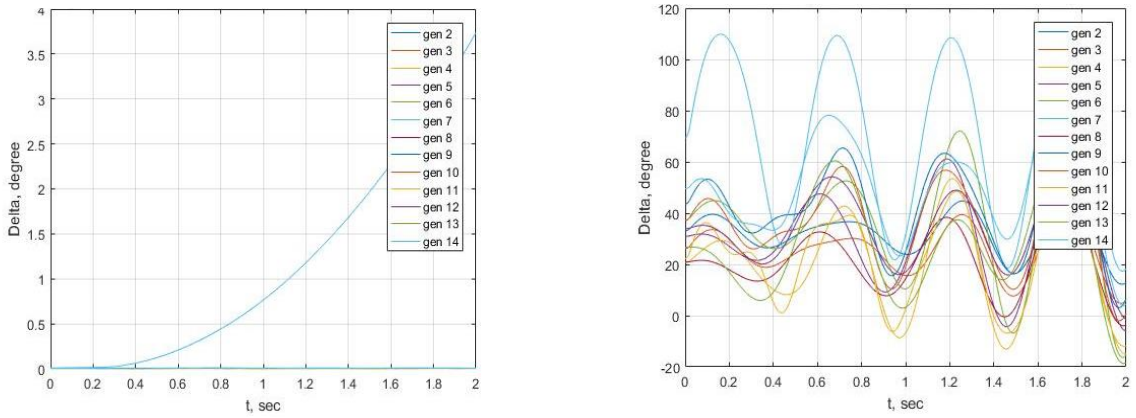

(a) (b)

Figure 8: Swing curve of three-phase fault on bus 20, line [15-20] of the Nigerian 34-power network and cleared at 0.021 s (a) without STATCOM (b) with STATCOM

Transient Stability Results for Three-Phase Fault on Bus 22, Line [22-29]

The peculiarity of bus 22 in the Nigerian 34-bus power network is that it was this bus that connected the largest generator in the system, Egbin with a total capacity of about 700 MVA. Although, it is expected that this generator because of its high capacity should not be perturbed by a fault in its vicinity and so, should maintain synchronism in the event of a fault. The swing curves for the three-phase short circuit fault introduced on bus 22, line [22-29] and cleared at different times with and without STATCOM are presented in Figures 9 to 11. Figures 9a and b revealed that the system was stable with and without compensation for a FCT of 0.013 s. The FCT increase to 0.0132 s without STATCOM resulted in generator 2 losing stability while generators 3 to 14 went into marginal stability as shown in Figure 10a. Figure 10b revealed that the application of STATCOM restored stability to the system. Instability on generator 2 persisted while generators 3 to 14 maintained marginal stability without STATCOM when the FCT increased further to 0.150 s as shown in Figure 11a but with compensation, stability was achieved in Figure 11b.

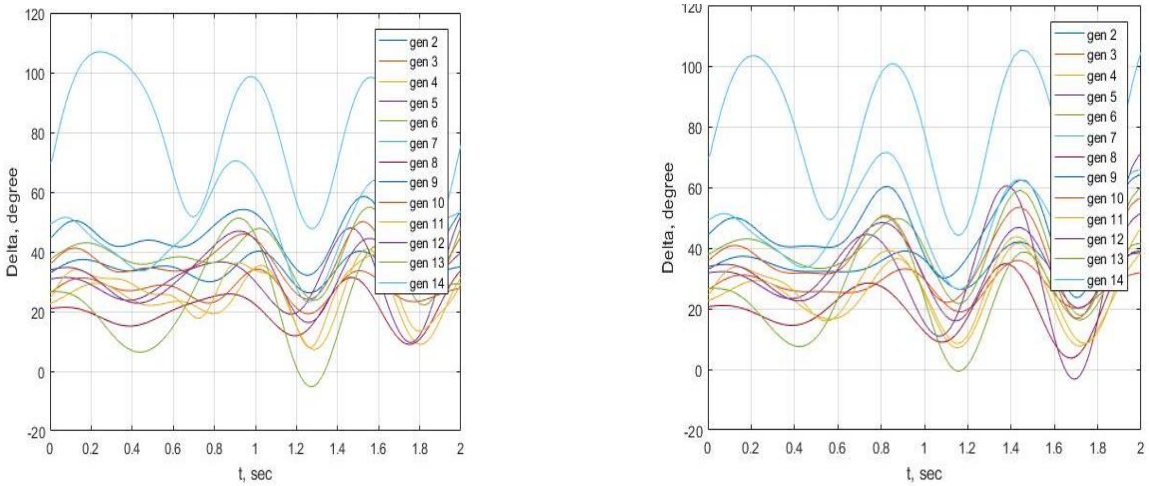

Figure 9: Swing curve of three-phase fault on bus 22, line [22-29] of the Nigerian 34-bus power network and cleared at 0.013 s (a) without STATCOM (b) with STATCOM

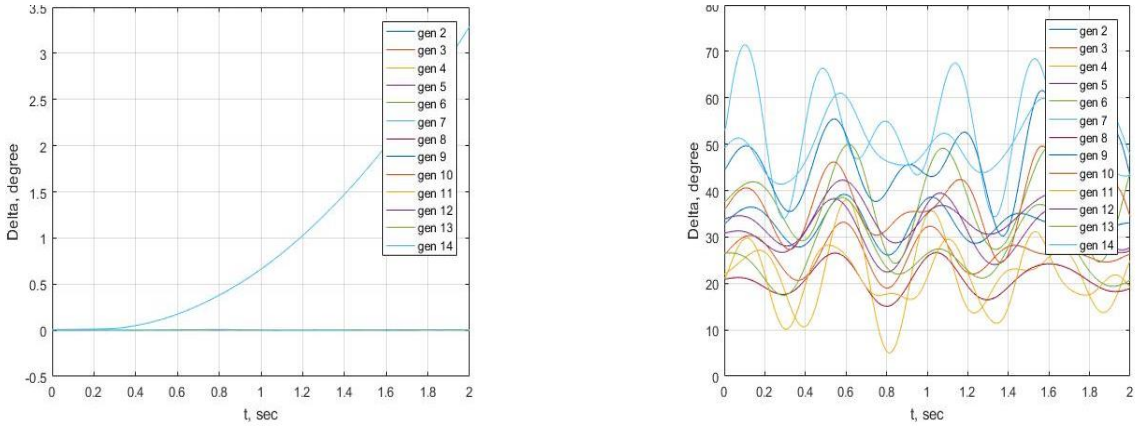

(a) (b)

Figure 10: Swing curve of three-phase fault on bus 22, line [22-29] of the Nigerian 34-bus power network and cleared at 0.0132 s (a) without STATCOM (b) with STATCOM

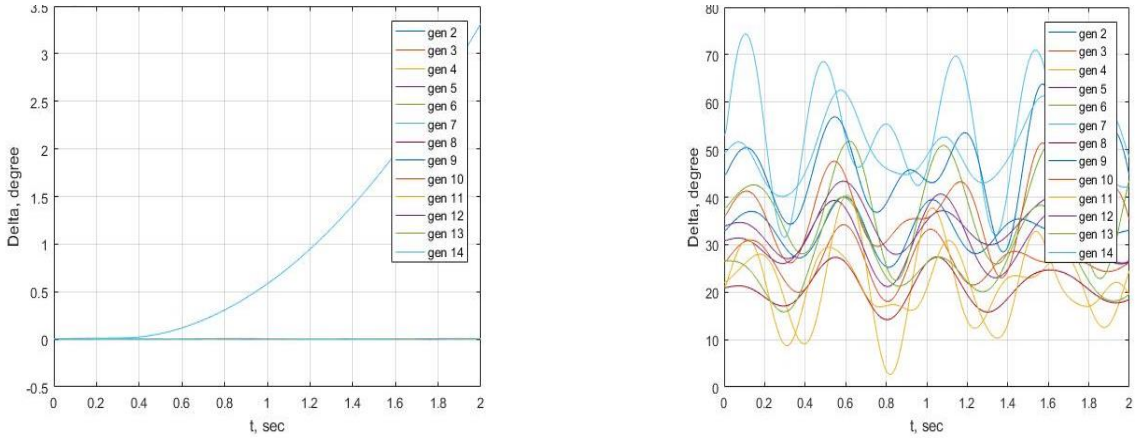

(a) (b)

Figure 11: Swing curve of three-phase fault on bus 22, line [22-29] of the Nigerian 34-bus power network and cleared at 0.0150 s (a) without STATCOM (b) with STATCOM

DISCUSSION OF THE RESULTs

In this study, transient stability analysis and enhancement were conducted on the Nigerian 34-bus network. The load flow analysis showed that the voltage magnitudes of Katampe, Kaduna T.S, Kano T.S, Jos T.S, and Gombe T.S which fell out of the voltage tolerance limit before compensation were improved with STATCOM inclusion. STATCOM through compensation of reactive power in the system mitigated the undervoltage conditions on the five constrained buses, thereby increasing their voltage magnitudes to be within the acceptable limit of operation. The improvement in voltage profile was also reflected in the total active line loss of the system which decreased by 4.03% with compensation from STATCOM.

Transient stability analysis for fault introduction on bus 20 (Akangba T.S) and bus 22 connecting Egbin, the largest specified generator in the Nigerian 34-bus power network before compensation revealed different behaviour of the system at different fault clearing times. In the case of the fault on bus 20, the system stability was negatively impacted when the FCT exceeded 0.019 s. Beyond 0.019 s, generator 14 lost synchronism completely while generators 2 to 13 maintained marginal stability, the conditions

which persisted a FCT of 0.021 s. The inclusion of STATCOM, however, extended the stability of the system beyond 0.019 s due to the compensation provided by the device to mitigate the effect of fault. A fault on bus 22 triggered marginal stability on Egbin (generator 7 on the swing curve) along with generators 3 to 6 and 8 to 14 while generator 2 completely lost synchronism for FCT exceeding 0.013 s up to 0.150 s. The STATCOM application, however, restored total stability to the system beyond 0.013 s where the stability of generators was observed to have been affected. The observed overall improvement in stability was a result of the compensating power of the STATCOM.

The results of transient stability improvement in this study are consistent with the findings of Jambulingam (2014) and Kale et al. (2018). Jambulingam (2014) and Kale et al. (2018) discovered in their respective findings that the STATCOM application was an appropriate technique for curtailing the transient instability of power networks. This submission is in tandem with the results obtained from the present study where it was found that the compensating ability of STATCOM extended the critical FCT of the considered system and stability maintained in the event of fault introduction.

CONCLUSION

The occurrence of major disturbances is inevitable in power system networks due to their complexity. One of the important steps usually undertaken to diagnose these systems so that synchronism is not lost is transient stability analysis. In this study, power system transient stability improvement via STATCOM was carried out considering the Nigerian 34-bus power networks. Power flow and swing equations modelling the system performance under steady state and transient conditions were formulated and simulated using a first principle coding process developed in MATLAB with and without compensation. A total of five buses were found to be constrained in the test network without STATCOM. Through compensation provided by the device, the voltage magnitudes on these constrained buses were improved and fell within the statutory voltage limit for effective operation.

The swing curves of the generators in the system with and without STATCOM revealed that stability in the event of fault was dependent on both the critical fault clearing time and the compensation provided by the FACTS device. A delay in fault clearing time caused some generators that were initially stable to become unstable while some experienced marginal stability when no STATCOM was installed on the systems. The use of STATCOM generally enhanced the stability of the system beyond the point at which some of the generators lost synchronism when the critical fault clearing time was exceeded as a result of the reactive power compensation provided by the device which catered for deficiencies at different points on the system. Hence, STATCOM provided the needed reactive compensation for transient stability improvement in the study. As a suggestion for further works in this area of the study, other versatile FACTS compensating devices such as SVC, SSSC, TCSC and UPFC could be deployed for transient stability enhancement and comparative evaluation with respective to STATCOM carried out. In addition, optimization approaches such as the use of fuzzy logic, genetic algorithm, artificial neural network, particle swarm optimization among other could be considered for optimal siting of the FACTS controllers for the improvement of transient stability on power system network.

REFERENCES

Adebisi, O. I., Adejumobi, I. A., Ogunbowale, P. E., & Ade-Ikuesan, O. O. (2018). Performance Improvement of Power System

Networks Using Flexible Alternating Current Transmission Systems Devices: The Nigerian 330 kV Electricity Grid as a Case Study. *LAUTECH Journal of Engineering and Technology*, *12*(2), 46–55.

Akpojedje, F. O., & Ogujor, E. A. (2021). Demand Side Management Strategy for Alleviating Power Shortages in Nigerian Power System : A Case Study. *Nigeria Journal of Technology*, *40*(5), 927–937. https://doi.org/10.4314/njt.v40i5.18

Anichebe, I. B., & Ekwue, A. O. (2020). Improvement of Bus Voltage Profiles of Nigerian Power Network in the Presence of Static Synchronous Compensator (STATCOM) and Doubly Fed Induction Generator (DFIG). *Nigerian Journal of Technology*, *39*(1), 228–237. https://doi.org/10.4314/njt.v39i1.26

Asare, P., Diez, T., Galli, A., O'Neill-Carillo, E., Robertson, J., & Zhao, R. (1994). Flexible AC transmission systems Part 2 methods of transmission line compensation. In *ECE Technical Report* (Vol. 205). https://doi.org/10.1049/pe:19960607

Azeez, T. T., & Abdelfattah, A. A. (2020). Transient Stability Enhancement and Critical Clearing Time Improvement for Kurdistan Region Network using Fact Configuration. *Journal of Engineering*, *26*(10), 50–65. https://doi.org/10.31026/j.eng.2020.10.04

Braide, S. L., & Diema, E. J. (2018). Analysis of Steady and Transients-State Stability of Transmission Network. *International Journal of Academic Research and Reflection*, *6*(5), 1–32.

Dobrushkin, V. (2024). *Mathematical Tutorial for the First Course, Part 1.3: Modified Euler Method*. https://www.cfm.brown.edu/people/dobrush/am33/mathematica/ch3/modify.html.

Eidiani, M., Ebrahimean Baydokhty, M., Ghamat, M., Zeynal, H., & Mortazavi, H. (2011). Transient stability enhancement via hybrid technical approach. *Proceedings - 2011 IEEE Student Conference on Research and Development, SCOReD 2011*, 375–380. https://doi.org/10.1109/SCOReD.2011.6148768

Eladany, M. M., Eldesouky, A. A., & Sallam, A. A. (2018). Power System Transient Stability: An Algorithm for Assessment and Enhancement Based on Catastrophe Theory and FACTS Devices. *IEEE Access*, *6*, 26424–26437. https://doi.org/10.1109/ACCESS.2018.2834906

Garg, L., Agarwal, S. K., & Kumar, V. (2017). Improvement of Transient Stability of IEEE 14 Bus System by using Series FACTS Controllers. *International Journal of Scientific & Engineering Research*, *8*(10), 280–286.

Glover, J. D., & Sarma, M. (2002). *Power System Analysis and Design with Personal Computer application*. PWS-KENT Publishing Company.

Gupta, J. B. (2011). *A Course in Power Systems*. S.K. Katari and Sons Publisher.

Gupta, K., & Pahariya, Y. (2017). Simulation Analysis of FACTs Devices for Transient Stability Improvement in Multi Machine System. *International Journal of Current Trends in Engineering & Technology*, *3*(1), 16–20.

Gupta, S., & Tripathi, R. K. (2015). Transient Stability Enhancement of Multi-Machine Power System using Robust and Novel Based CSC-STATCOM. *Advances in Power Electronics*, *2015*, 626731. https://doi.org/10.1155/2015/62671

Hadi, S. (2008). *Power System Analysis*. McGraw-Hill Companies, Inc.

Igwilo, O. C., Oodo, O., Nnabugwu, C. P., Ojikpong, G. K., Anyasi, P. O., & Adesina, I. A. (2021). An Overview of the Composite Design of Smart Grid due to Power Demand, Production and Power Deficit in Nigeria. *Asian Journal of Engineering and Technology*, *9*(4), 71–80. https://doi.org/10.24203/ajet.v9i4.6617

Ikeli, H. N. X. (2019). *A Critical Analysis of Transient Stability of Electrical Power System: A Case Study of Nigerian 330 kV Power System*. M.Eng. Dissertation. University of Nigeria, Nsukka.

Jambulingam, V. (2014). Power System Stability Improvement Under Three Phase Faults Using Static Synchronous Compensator.

International Journal of Research in Engineering and Technology, *3*(7), 89–97. https://doi.org/10.15623/ijret.2014.0307015

Jokojeje, R. A., Adejumobi, I. A., Adebisi, O. I., & Mufutau, W. O. (2015a). Reactive Power Compensation in Nigeria Electricity Grid Using Static Reactive Power Compensation in Nigeria Electricity Grid Using Static Synchronous Compensator (STATCOM). *IOSR Journal of Electrical and Electronics Engineering*, *10*(2), 8–20. https://doi.org/10.9790/1676-10240820

Jokojeje, R., Adejumobi, I., Mustapha, A., & Adebisi, O. (2015b). Application of Static Synchronous Compensator (STATCOM) in Improving Power System Performance: A Case Study of The Nigeria 330 KV Electricity Grid. *Nigerian Journal of Technology*, *34*(3), 564. https://doi.org/10.4314/njt.v34i3.20

Kakaiya, S., & Parekh, D. B. (2019). Transient Stability Improvement Using STATCOM. *3rd International Conference on "Advances in Power Generation from Renewable Energy Sources" 2019*, 1–9. https://doi.org/10.2139/ssrn.3442558

Kale, K., Meshram, A., Sathawane, R., & Jethani, S. (2018). Power System Stability Improvement Using STATCOM. *International Journal of Latest Tecnology in Engineering*, *7*(3), 90–93.

Khan, N., Ahmad, H., & Khattak, A. (2017). Transient Stability Enhancement of Power System using UPFC (Unified Power Flow Controller). *International Journal of Engineering Works*, *4*(2), 33–40. www.kwpublisher.com

Kothari, D. P., & Nagrath, I. J. (2008). *Power System Engineering* (Second Edi). Tata McGraw-Hill Publishing Company Limited.

Kumar, S. V. R., & Nagaraju, S. S. (2007). Transient Stability Improvement using UPFC and SVC. *ARPN Journal of Engineering and Applied Science*, *2*(3), 38–45.

Mumtahina, U., Alahakoon, S., & Wolfs, P. (2023). A Literature Review on the Optimal Placement of Static Synchronous Compensator (STATCOM) in Distribution Networks. *Energies*, *16*, 6122. https://doi.org/10.3390/en16176122

Murali, D., Rajaram, M., & Reka, N. (2010). Comparison of FACTS Devices for Power System Stability Enhancement. *International Journal of Computer Applications*, *8*(4), 30–35. https://doi.org/10.5120/1198-1701

Ogboh, V. C., Chibueze, K., Anyalebechi, A. E., Ogboh, V. C., Obute, K. C., & Anyalebechi, A. E. (2019). Transient Stability Analysis of Power Station (A Case Study of Nigeria Power Station). *The International Journal of Engineering and Science (IJES)*, *7*(8), 23–42. https://doi.org/10.9790/1813-0708022842

Okakwu, I. K., & Ogujor, E. A. (2017). Enhancement of Transient Stability of the Nigeria 330 kV Transmission Network Using Fault Current Limiter. *Journal of Power and Energy Engineering*, *05*(09), 92–103. https://doi.org/10.4236/jpee.2017.59008

Padiyar, K. R., & Rao, U. K. (1999). Modeling and Control of Unified Power Flow Controller for Transient Stability. *Electrical Power and Energy*, *21*, 1–11.

Qader, M. R. (2015). Design and Simulation of a Different Innovation Controller-Based UPFC for the Enhancement of Power Quality. *Energy*, *89*, 576–592.

Ramana, G., & Ram, B. V. S. (2011). Power System Stability Improvement Using Facts With Expert Systems. *International Journal of Advances in Engineering & Technology*, *1*(4), 395–404.

Samsudin, N., Yusop, N. M. M., Nasir, A., Sulaiman, N. S., & Zulkifli, N. S. (2021). Euler Root Mean Square (ERMS): A New Modified Euler Method to Improve Accuracy of Resistor-Inductor (RL) Circuit Equation. *Journal of Physics: Conference Series*, *1874*(1), 012039. https://doi.org/10.1088/1742-6596/1874/1/012039

Shrivastava, M., Prakash, V., Kaushik, V., & Upadhyay, V. K. (2021). Transient Stability Improvement of IEEE 9-Bus System Using Static Var Compensator. *International Journal of Research in Engineering, Science and Management*, *4*(4), 98–102.

https://doi.org/10.47607/ijresm.2021.663

Singh, B., Verma, K. S., Mishra, P., Maheshwari, R., Srivastava, U., & Baranwal, A. (2012). Introduction to FACTS Controllers : A Technological Literature Survey. *International Journal of Automation and Power Engineering*, *1*(9), 193–234.

Udo, J. F., & Aminu, M. A. (2019). Transient Stability Improvement on Jos – Gombe 330kV Line Using Static Var Compensator. *Journal of Scientific Research and Reports*, *24*(5), 1–7. https://doi.org/10.9734/jsrr/2019/v24i530166

APPENDICES

I: Bus Parameters of the Nigeria 34-Bus, 330 kV Power System Network

Bus No	Bus Type	Pd (MW)	Qd (MVAr)	Vm (p.u.)	Vmax (p.u.)	Vmin (p.u.)
1	3	00.00	00.00	1.06	1.05	0.95
2	1	40.00	- 10.00	1.0	1.05	0.95
3	2	00.00	00.00	1.04	1.05	0.95
4	1	140.00	30.00	1.0	1.05	0.95
5	1	90.00	30.00	1.0	1.05	0.95
6	1	160.00	70.00	1.04	1.05	0.95
7	2	00.00	00.00	1.0	1.05	0.95
8	1	130.00	70.00	1.0	1.05	0.95
9	1	300.00	90.00	1.0	1.05	0.95
10	1	210.00	40.00	1.02	1.05	0.95
11	2	00.00	00.00	1.0	1.05	0.95
12	1	50.00	-20.00	1.0	1.05	0.95
13	1	100.00	-30.00	1.0	1.05	0.95
14	1	120.00	60.00	1.0	1.05	0.95
15	1	500.00	50.00	1.0	1.05	0.95
16	1	250.00	43.00	1.0	1.05	0.95
17	1	70.00	38.00	1.0	1.05	0.95
18	2	00.00	00.00	1.03	1.05	0.95
19	1	200.00	55.00	1.0	1.05	0.95
20	1	150.00	35.00	1.0	1.05	0.95
21	2	00.00	00.00	1.02	1.05	0.95
22	2	00.00	00.00	1.05	1.05	0.95
23	1	300.00	45.00	1.0	1.05	0.95
24	2	00.00	00.00	1.04	1.05	0.95
25	1	100.00	58.00	1.0	1.05	0.95
26	2	00.00	00.00	1.01	1.05	0.95
27	2	00.00	00.00	1.03	1.05	0.95
28	2	00.00	00.00	1.02	1.05	0.95
29	1	120.00	80.00	1.0	1.05	0.95
30	1	130.00	-78.00	1.0	1.05	0.95
31	2	00.00	00.00	1.03	1.05	0.95
32	1	200.00	67.00	1.0	1.05	0.95
33	2	00.00	00.00	1.04	1.05	0.95

34	2	00.00	00.00	1.02	1.05	0.95

II: Generator Parameters of the Nigeria 34-Bus, 330 kV Power System Network

Bus No	**Pg (MW)**	**Qg (MVAr)**	**Qmax (MVAr)**	**Qmin (MVAr)**	**Vg (p.u.)**	**R (p.u.)**	**X (p.u.)**	**H**
1	00.00	00.00	0	0	1.05	0.0020	0.0901	9.920
3	300.00	40.00	110	0	1.04	0.0080	0.3000	3.390
7	400.00	60.00	140	0	1.0	0.0240	0.3000	3.240
11	150.00	50.00	114	0	1.0	0.0036	0.2200	4.000
18	280.00	45.00	100	0	1.03	0.0020	0.1240	12.400
21	240.00	55.00	104	0	1.02	0.0036	0.2200	4.000
22	700.00	68.00	108	0	1.05	0.0040	0.3080	3.090
24	180.00	00.00	132	0	1.04	0.0030	0.1060	12.690
26	190.00	-35.00	126	0	1.01	0.0061	0.3400	1.245
27	150.00	51.00	100	0	1.03	0.0036	0.3000	1.242
28	130.00	80.00	150	0	1.02	0.0051	0.2100	1.249
31	150.00	00.00	100	0	1.03	0.0061	0.3000	4.000
33	200.00	59.00	140	0	1.04	0.0010	0.0610	28.050
34	300.00	65.00	125	0	1.02	0.0051	0.1900	1.350

III: Branch Parameters of the Nigeria 34-Bus, 330 kV Power System Network

From Bus	**To Bus**	**R (p.u.)**	**X (p.u.)**	**B (p.u.)**
1	2	0.0121836	0.0916336	1.21
1	4	0.0015918	0.0119716	0.31
3	4	0.0001572	0.0094178	0.00
4	5	0.0047827	0.0360219	0.09
4	9	0.0020565	0.0154692	0.07
5	6	0.0018864	0.0141884	0.36
5	7	0.0003144	0.0188355	0.00
5	10	0.0018864	0.0141884	0.37
8	9	0.0053843	0.0404961	0.33
8	15	0.0053343	0.0405651	0.45
9	15	0.0065432	0.0426547	0.55
9	16	0.0098648	0.0741936	0.98
10	13	0.0090394	0.0679862	0.52
10	14	0.0077425	0.0582316	0.77
11	15	0.0020643	0.0103951	0.31
12	15	0.0040534	0.0305160	0.41
14	17	0.0104150	0.0783319	0.01
15	16	0.0110045	0.0827653	0.09
15	20	0.0003527	0.0026574	0.05
15	21	0.0055023	0.0413829	0.35

15	22	0.0012184	0.0091634	0.20
16	18	0.0063843	0.0404961	0.15
16	19	0.0038336	0.0288242	0.76
16	21	0.0055023	0.0413829	0.55
16	23	0.0053843	0.0404961	0.38
16	24	0.0009826	0.0073898	0.19
18	25	0.0010218	0.0076553	0.10
19	26	0.0005109	0.0038427	0.38
19	27	0.0006105	0.0038427	0.40
22	28	0.0005109	0.0036458	0.30
22	29	0.0002749	0.0020654	0.20
23	30	0.0037730	0.0283768	0.37
23	31	0.004913	0.0036949	0.09
23	32	0.00605225	0.0455212	0.02
24	25	0.0024760	0.0186223	0.24
28	29	0.0034640	0.0206114	0.30
32	33	0.0009825	0.0073898	0.09
33	34	0.0005109	0.0038427	0.30